Available online at www.sciencedirect.com
ScienceDirect
Ceramics International 35 (2009) 585–590
CERAMICS INTERNATIONAL
www.elsevier.com/locate/ceramint

Densification behaviour and microstructural evolution of TiO_2/CAS-incorporated alumina

Chen Chang-ping, Yang Hui-zhi, Gao Jing-xia, Sun Hong-wei, Hu Xing *

School of Physical Engineering and Material Physics Laboratory, Zhengzhou University, Zhengzhou 450052, China

Received 15 March 2007; received in revised form 8 July 2007; accepted 12 January 2008
Available online 24 April 2008

Abstract

Densification behaviour and microstructural evolution of TiO_2/CAS (CaO-Al_2O_3-SiO_2)-incorporated alumina has been investigated systematically. The experimental results show that TiO_2 can greatly enhance the densification rates of alumina but trigger severely abnormal grain growth (AGG) at 0.60 wt%. On the other hand, small amounts of CAS can effectively inhibit abnormal grain growth, but provoke an abnormal densification owing to the formations of in situ pores left by liquid phase. With additional 0.50 wt% of CAS incorporated into 0.60 wt% TiO_2-doped sample, the aspect-ratios of anisotropic growth grains increase by reduced growth rates of flat boundaries, accomplished by basal planes much smoother and straighter. This microstructure subsequently disappears when CAS incorporation is up to 4.0 wt%, substituted by that with low aspect-ratio and fine-equiaxed grains. Such occurrences are discussed in term of levels of liquid phase and 2-dimension (2-D) nucleation processes.

Keywords: Densification; Microstructure; Alumina; Abnormal grain growth

1. Introduction

Incorporating a certain amounts of sintering additives into alumina has been confirmed to be an effective way to lower its sintering temperature and modify its microstructures [1–4]. This method, including adding solid-solution additives, such as TiO_2, MnO_2 or Cr_2O_3 [4–7] as well as adding liquid-phase forming additives, such as R_2O-Al_2O_3-SiO_2 or $R'O$-Al_2O_3-SiO_2 (where R and R′ represent atoms of alkali and alkaline-earth metals, respectively) [4,8], etc., has been widely studied and employed in practical applications.

TiO_2 is one of the most typical solid-solution additives, which can be dissolved in alumina at high temperature to promote the sintering process though vacancy diffusion mechanism. However, excessive additions of TiO_2 may cause the formation of a second phase of Al_2TiO_5 at the grain boundary, which may subsequently inhibit the densification of alumina [5,9,10]. Moreover, abnormal grain growths (AGG) can be observed frequently within the matrix, which are assumed to be associated with the emergence of small amounts of liquid phase and a 2-dimensional (2-D) nucleation process during sintering [11–14].

Comparatively, CaO-Al_2O_3-SiO_2 system has been considerably investigated among the RO-Al_2O_3-SiO_2 type, owning to its relatively low melting-temperature and high solubility in alumina [4]. Up to 20 wt% of CAS incorporation may reduce sintering temperature of alumina to about 1500 °C without significant compromising of mechanical properties, therefore having been widely used in industry up to date. Although AGG readily occur in alumina with either high or low concentration of CAS [15,16], such growth kinetics are effectively avoided by adjusting levels of liquid phase or/and doping inhibitor of MgO simultaneously [17,18].

Some of previous studies were intentionally focused on the combined effects of additives, such as TiO_2-MnO_2 [19], MgO-FeO [20], and CaO/SiO_2-MgO [21], on sintering behaviours of alumina. Favorable densification or/and controllable microstructure is always achieved with such additives in a certain proportion. Based on the prominent effects of TiO_2 and CAS on alumina, densification behaviour and microstructure evolution are systematically studied in this work, employing deliberately above two types of sintering mechanisms.

* Corresponding author. Tel.: +86 37167767671; fax: +86 37167766629.
E-mail address: xhu@zzu.edu.cn (H. Xing).

0272-8842/$34.00
doi:10.1016/j.ceramint.2008.01.024

2. Experimental procedure

Commercially available Al_2O_3 powders (purity 99.9%, average grain size of 0.1 μm, MC2A, Chengsheng Ltd., Zhejiang, China) as well as reagent grade CaO, Al_2O_3, SiO_2, and TiO_2 were used as the starting materials. According to the lowest eutectic compositions in the CaO-Al_2O_3-SiO_2 system, a mixed power of 23.7% CaO, 14.3% Al_2O_3 and 62.0% SiO_2 by weight was melted at 1450 °C for 2 h, and then quenched in water to pre-synthesize CAS glass. The transparent glass was crushed less than 0.5 mm in a mortar, following by sieving through 100-μm screen after wet-milling for 10 h with high purity alumina media.

Thirty different compositions in this study were prepared according to combinations of TiO_2 and CAS, in which TiO_2 levels were fixed at 0, 0.15 wt%, 0.30 wt%, 0.45 wt%, 0.60 wt%, 1.00 wt%, while CAS levels at 0, 0.5 wt%, 1.0 wt%, 2.0 wt%, and 4.0 wt%, respectively. Contrary to colloidal processing routes, TiO_2 and as-received CAS were directly incorporated into alumina as sintering aids and wet-milled in ethanol for 3 h again in a planetary ball mill. The slurry was dried with continuous stirring to prevent the sedimentation, sieved through a 100-μm screen, and then softly ground with mixed solution of PVA and PEG. The powders were uniaxially pressed into pellets at 150 MPa after sieved through a 400-μm screen, and subsequently sintered at 1550 °C for 2 h at a heating rate of 5 °C/min.

Bulk densities of samples were determined by Archimedes method. Surfaces of samples were polished by machine with diamond pastes of down to 0.5 μm, and then thermally etched at 1450 °C for 1 h to reveal grain boundaries for microscopic examinations. Microstructures of samples were examined by scanning electron microscopy (SEM, Model JSM-6700, JEOL, Tokyo, Japan) equipped with X-ray energy dispersive spectroscopy (EDS). Sample with 4.0 wt% CAS was broke up in a high purity alumina mortal to obtain powders. Phase analysis of as-received powders and thermally etched surfaces were carried out by X-ray diffraction (XRD, Philips X'Pert PRO, Almelo, Netherland). Mean linear intercept, L, was determined from SEM image of sample containing more than 200 grains. Average grain size was calculated by convention $G = 1.5 \times L$.

3. Results and discussions

3.1. Densification behaviours

Relative bulk densities of sintered samples are plotted in Fig. 1 as functions of TiO_2 and CAS concentrations. As can be observed, densifications of samples are complicated by the simultaneous incorporation of TiO_2 and CAS, which is assumedly due to the combined effects of solid-solution and liquid-phase sintering. Less than 0.30 wt% of TiO_2 can effectively accelerate densification rates of alumina, causing the samples to achieve about 95% of theoretic density (TD, 3.98 g/cm^3). Such sintering behaviours, however, become gradually reversed when CAS concentrations are added up to

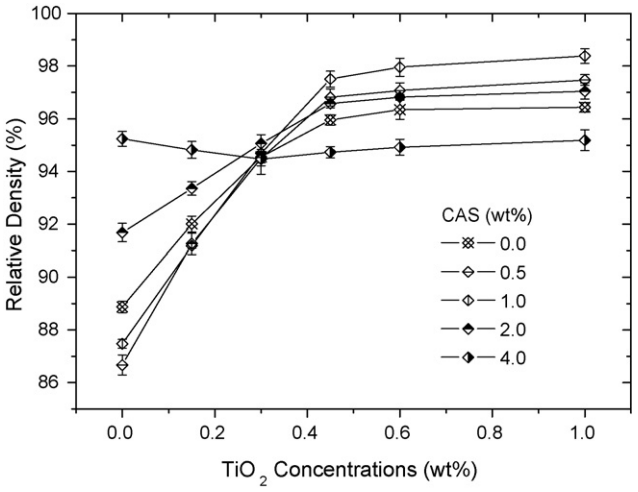

Fig. 1. Relative bulk densities of sintered simples incorporated with TiO_2 and CAS.

4.0 wt%, above which densifications appear to decrease with increasing TiO_2 concentrations. On the other hand, note that it is the large (≥2.0 wt%) rather than small (≤0.5 wt%) amounts of CAS that can increase the densities of samples at same levels of TiO_2-doping. Such experimental results obviously suggest that both liquid phase of CAS and solid-solution of TiO_2 play significant roles in determining sintering processes of low levels of TiO_2-doped alumina.

Interestingly, densification distinctions resulting from the different liquid-phase levels tend to be gradually undistinguished with TiO_2 increasing from 0 wt% to 0.30 wt%. Especially when TiO_2 concentration is equal to 0.3 wt%, all samples are approximately 94.5% of TD, despite additions of CAS ranging between 0 wt% and 4.0 wt%. This may indicate that the solid-solution of TiO_2 dominates the densification processes during sintering. However, such sintering behaviours change again when TiO_2 is beyond 0.3 wt%. Bulk densities further increase with the increase of TiO_2 until TiO_2 reaches 0.45 wt%. Beyond this value, there is almost no obviously further increase of density when TiO_2 concentrations vary from 0.45 wt% to 1.0 wt%, whereas CAS liquid phase appears to acts as important roles during sintering.

In temperature range of 1300–1700 °C in air, the solubility of TiO_2 in alumina has been reported to be around 0.27 wt% and the solubility is grain size dependent with a higher level in finer particles. The favorable addition of TiO_2 to promote the densification approximately matches its solubility in alumina, beyond which sintering kinetics may be leveled off due to formation of second phase at grain boundary [9,22,23]. In this work, however, more than 0.45 wt% of TiO_2 was found to favor the sintering and there seem no signs of decreased densification with further additions, which are not well consistent with some of studies. These may be explained by the direct incorporation instead of colloidal process of TiO_2 employed in this work, which lead to the agglomerations and heterogeneous distribution of TiO_2 within entire matrix.

Fig. 2 shows the contour lines of relative densities of sintered samples versus the concentrations of TiO_2 and CAS. According

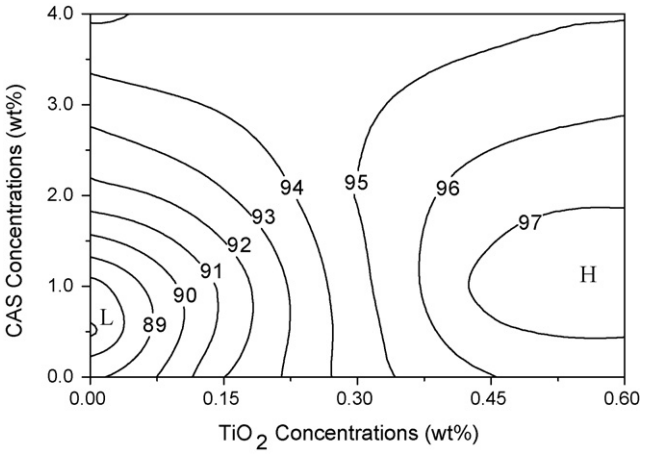

Fig. 2. Contour lines of densification of alumina incorporated with TiO_2 and CAS.

to the analyses of Fig. 1, only the representative parts of diagram with $TiO_2 \leq 0.6$ wt% were given in the present study.

As can be clearly seen from Fig. 2, two distinct areas, L with relatively low densities as well as H with relatively high densities, respectively, are found with bulk densities varying with gradient from 87% to 98% of TD. The contour lines within L area seems more denser than those within H, which implies that a small rather than large amounts of additives have more pronounced effects on densification of alumina. Abnormal densification behaviours are also observed within L area. The 0.5 wt% CAS-doped sample reaches only about 86.7% of TD, which is even a little lower than that (88.9%) of the sample incorporating neither TiO_2 nor CAS. Contrary to such observations, enhanced sintering behaviours occur within H area, with high densities for sample incorporating about 0.6 wt% TiO_2 and 1.0 wt% CAS. In the middle areas between L and H, notably nearby the compositions with 0.3 wt% TiO_2, densifications are not affected much by additions of CAS, which is consistent with observations in Fig. 1. Some of above-described experimental phenomena will be discussed in detail below in term of the microstructures of TiO_2/CAS-incorporated samples.

3.2. Microstructural evolutions

SEM images of samples that were singly incorporated with 0.5 wt% and 4.0 wt% CAS are shown in Fig. 3(a) and (b), respectively. As can be seen clearly, no obvious evolutions of AGG are observed in two samples, which show an approximately grain size distributions with ~2.5 μm average grain size. However, grain morphologies as well as pore sizes and distributions can be clearly discerned with varying liquid phases. Comparatively, non-uniform densification occurs in

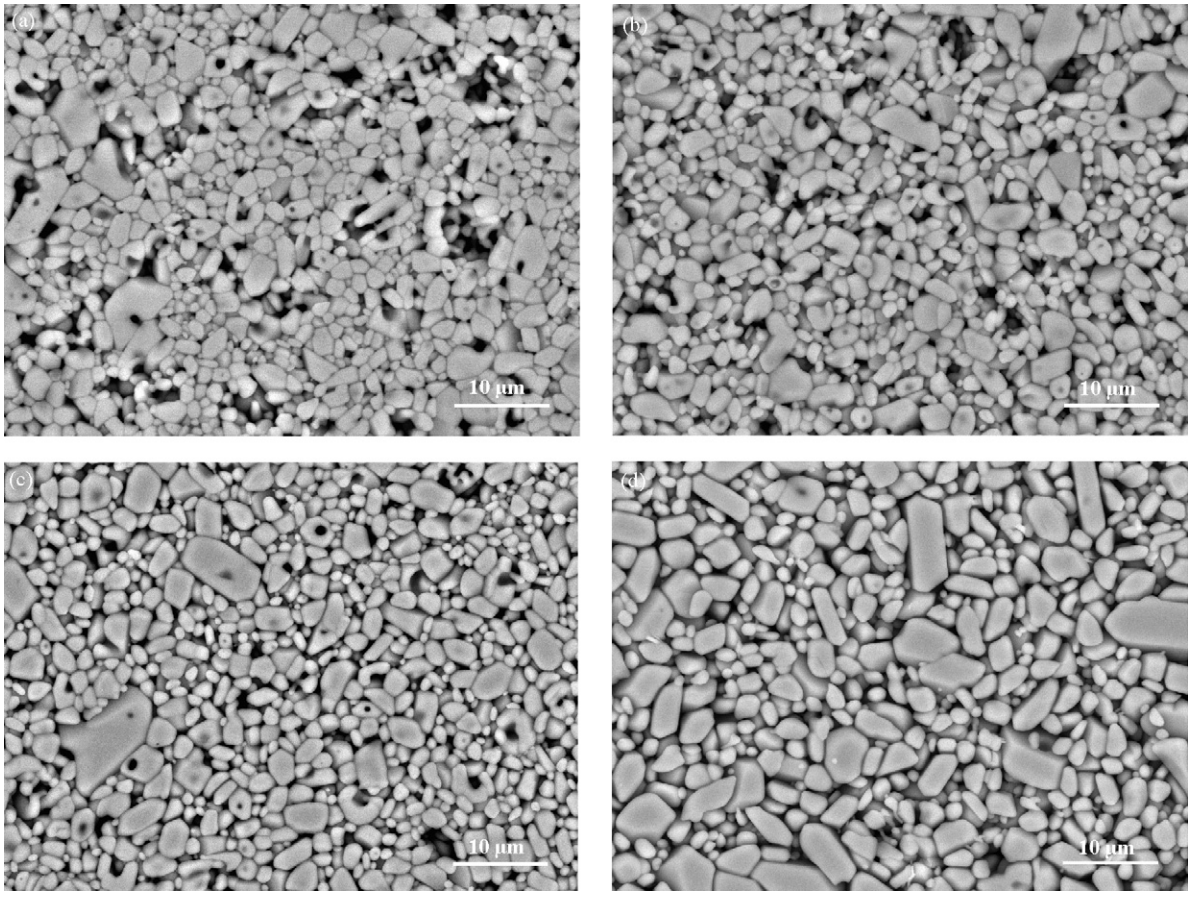

Fig. 3. SEM images of singly CAS incorporated as well as CAS and TiO_2 co-incorporated samples: (a) 0.5 wt% CAS; (b) 4.0 wt% CAS; (c) 0.5 wt% CAS–0.15 wt% TiO_2; (d) 4.0 wt% CAS–0.15 wt% TiO_2.

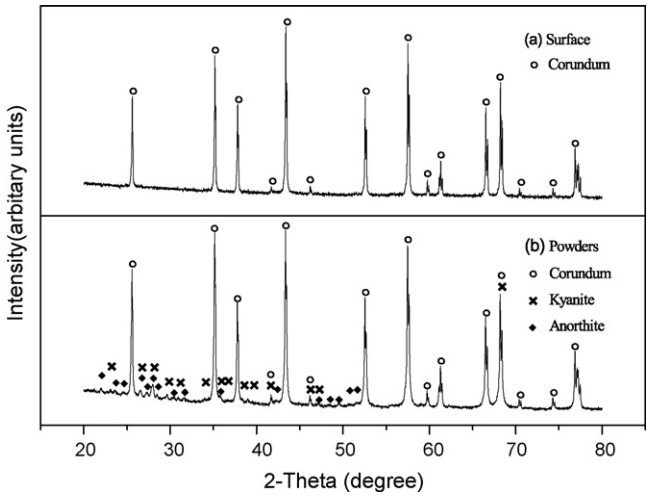

Fig. 4. XRD patterns of sample with 4.0 wt% CAS: (a) surface and (b) powders, respectively.

0.5 wt% CAS-incorporated sample. Large size pores are distributed in locally dense matrix, causing this sample no more than 86.7% of TD as observed in Fig. 2. At the same time, the grains exhibit a tendency to become spherical when liquid phase content increases to 4.0 wt%, as shown in Fig. 3(b). Such occurrences resulted presumably from the characteristics of liquid-phase sintering in the presence of CAS.

In general, densification of compacts with small amounts of liquid phase is of transient liquid-phase sintering process and distinct apparently from that of classical liquid-phase sintering model originally proposed by Kingery and Narasimhan [24,25]. Rearrangement of particles almost contributes little to densification, since liquid phases are insufficient to distribute within entire matrix [26]. Large pores can be left in situ once the liquid phases flow between grain boundaries via capillary force, which are experimentally examined from 0.5 wt% CAS-incorporated sample (Fig. 3(a)). However, typical liquid-phase sintering processes will take place as liquid phase concentrations approach to a critical level. The enhanced densification can be always achieved by extensive rearrangement, solution-precipitation, and coalescence of liquid-phase sintering, accompanied by alumina grains spherically coarsen (Fig. 3(b)).

Note that there are no obvious liquid phase or second phases observed in SEM images, whereas CAS concentrations reach up to 4.0 wt%. XRD analysis was then performed on the surfaces of sample that was polished and thermally etched at 1450 °C for 1 h. In addition to corundum crystalline phase, no liquid phase or other second phases can be found in the microstructure (Fig. 4(a)), which is consistent with the naked-eye observations in Fig. 3(b). Taking account of possible melting and evaporating of liquid phase or second phases from surface during thermally etching, bulk sample was broke up to obtain the sintered powders. The as-received powders were then

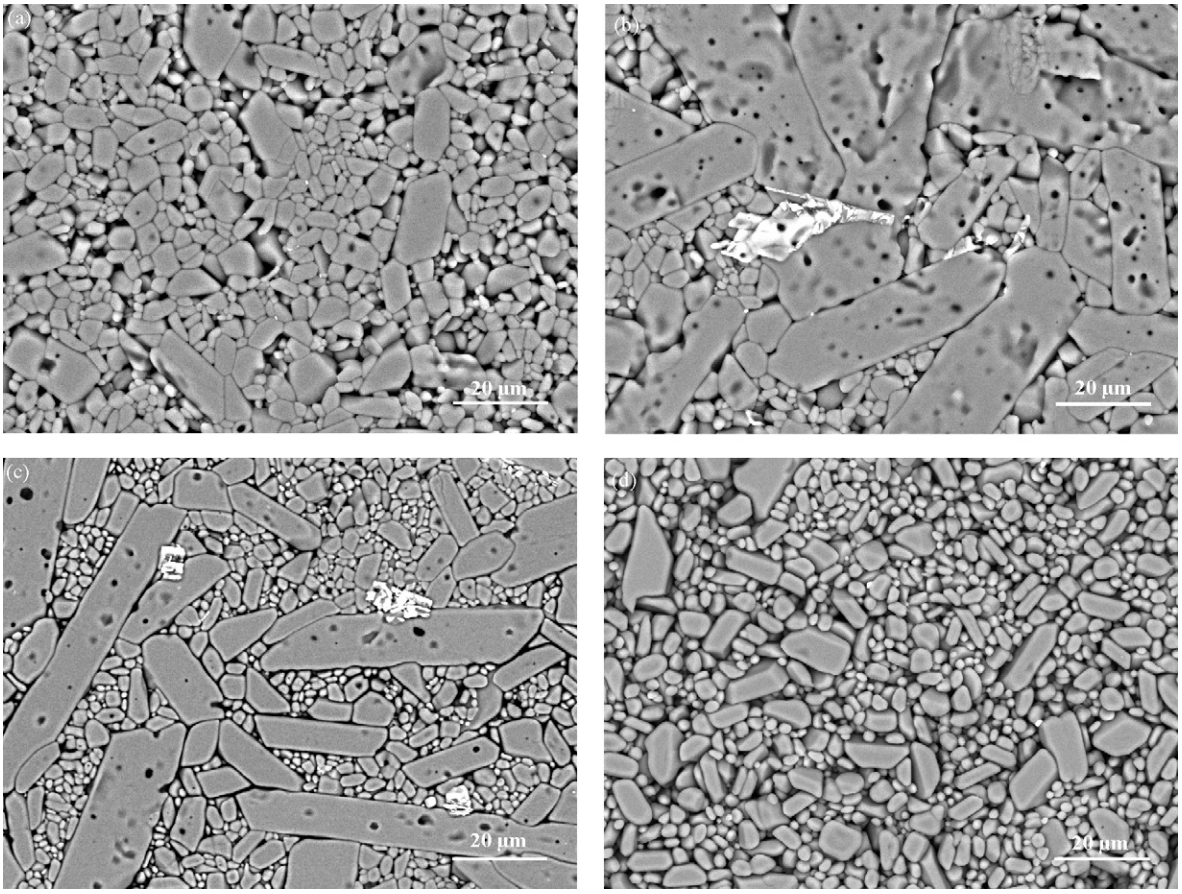

Fig. 5. SEM images of singly TiO_2 incorporated as well as TiO_2 and CAS co-incorporated samples: (a) 0.3 wt% TiO_2; (b) 0.6 wt% TiO_2; (c) 0.6 wt% TiO_2–0.5 wt% CAS; (d) 0.6 wt% TiO_2–4.0 wt% CAS.

examined by XRD. The results have indicated that in addition to the major phase of corundum, small amounts of other crystalline phases, such as anorthite ($CaAl_2Si_2O_8$) and kyanite (Al_2SiO_5), were also detected (Fig. 4(b)), which come from the reactions of CAS with Al_2O_3.

Furthermore, the microstructures of samples with varying CAS can be affected by incorporations of additional 0.15 wt% TiO_2. Compared with 0.5 wt% CAS-incorporated sample, grain size distribution is still kept constant in 0.5 wt% CAS–0.15 wt% TiO_2 co-incorporated sample, except for few of abnormal growth grains randomly dispersed in matrix (Fig. 3(c)). Large pores, however, have been removed from the compact, which seem a little denser than that with only 0.5 wt% CAS. On the contrary, enhanced grain growths and bimodal grain size distributions are observed in 4.0 wt% CAS–0.15 wt% TiO_2 co-incorporated sample (Fig. 3(d)). The sample with ~4 μm average grain size consists of relatively large elongated grains with low aspect-ratios and fine-equiaxed grains with ~2.5 μm in size. In this respect, AGG are suggested to be initiated with 4.0 wt% CAS–0.15 wt% TiO_2.

Compared with CAS incorporating, small amounts of singly TiO_2-doping appears to have more pronounced effects on microstructures of alumina. AGG was not severely triggered in 0.3 wt% TiO_2-doped sample. Relatively large elongated grains of ~20 μm in length and ~10 μm in thickness are dispersed within ~4 μm fine-equiaxed matrix grains (Fig. 5(a)). However, typically AGG occur in 0.6 wt% TiO_2-doped sample, resulting in grain size distributions extremely bimodal (Fig. 5(b)). Large elongated grains with ~40 μm in length and ~20 μm in thickness dominate the microstructures, together with ~4 μm fine-equiaxed grains agglomerated in matrix. The flat boundary perpendicular to thickness direction has been confirmed to be the basal (0 0 0 1) plane in previous studies [27]. Note that the migrations of non-basal planes migrate so fast during sintering that not only pores but also grains were trapped in anisotropic growth grains. In addition, small amounts of second phases within microstructure, which are clearly shown in Fig. 5(b), are identified by EDS as TiO_2 and Al_2TiO_5. Such observations are probably originated from the inhomogeneous distribution, segregation and/or precipitation of TiO_2 in matrix.

In contrast with additional 0.15 wt% TiO_2 influencing microstructures of varying amounts of CAS-incorporated samples, liquid phase of CAS seems to play more decisive roles in grain growth kinetics of 0.6 wt% TiO_2-doped sample. Small amounts of additional 0.5 wt% CAS incorporation are found to increase the average aspect-ratio of anisotropic growth grains by a factor of about two by reducing the half length while keeping the approximately length, as nicely shown in Fig. 5(c). At the same time, the basal plane obviously appears much smoother or straighter, compared with a little curved interface of AGG in Fig. 5(b). Nevertheless, such microstructures with much higher aspect-ratio and flatter planes disappear when liquid phase of CAS increase to 4.0 wt%, substituted by those with low aspect-ratio grains and ~4 μm fine-equiaxed grains, which is clearly shown in Fig. 5(d).

It should be noted that the average grain size in 0.6 wt% TiO_2–4.0 wt% CAS co-incorporated sample is ~8 μm and about two times larger than those of 0.15 wt% TiO_2–4.0 wt% CAS co-incorporated sample ((Fig. 3(d)), whereas the grain size distributions of two samples appear seemingly similar (Notice the different magnifications for two samples.) Such observations indicate that grain growth kinetics of alumina are still enhanced by TiO_2 incorporations, although large amounts of liquid phase of CAS can remarkably suppress AGG triggered by doping 0.6 wt% TiO_2.

AGG are generally assumed to be correlated with 2-D nucleation processes and uneven distributions of small amounts of liquid phase. According to Kim et al. [14,28], liquid phase are more possible in the presence of basal plane than non-basal plane, and thus grain boundary re-entrant edges (GBRE) are frequently formed at partially wetted non-basal planes. Since the 2-D nucleation barrier at GRRE is much lower than that at the basal planes, AGG can be initiated by non-basal planes migrating much faster than basal planes. In the present study, 0.5 wt% CAS can effectively reduce the growth rates of flat boundaries of AGG presumably by increasing corresponding probabilities of liquid phase in the presence of basal planes. However, AGG are strongly inhibited when CAS is incorporated up to 4.0 wt%. In this respect, it is expected that the planes of alumina grains, whether basal or non-basal, are all covered with liquid, which in turn show no obvious anisotropic growth behaviours.

4. Conclusions

Densification behaviours and microstructure evolutions of alumina during sintering are complicated by simultaneous incorporations of TiO_2 and CAS glass. Low concentrations of 0.5 wt% CAS can effectively inhibit AGG, but result in abnormal densification behaviours due to the formations of in situ pores left by insufficient liquid phase. On the other hand, small amounts of TiO_2 can greatly enhance densification rates, but trigger severely AGG at 0.60 wt%. However, the kinetics of AGG changes with varying amounts of additional CAS. When small amounts of 0.5 wt% CAS are incorporated 0.6 wt% TiO_2-doped sample, growth rates of flat boundaries of AGG are reduced by a factor of about two presumably by increasing probabilities of liquid phase in the presence of basal planes. When CAS increases up to 4.0 wt%, all planes of alumina grains, whether basal or non-basal, are totally covered with liquid, which in turn show no obvious anisotropic growth behaviours.

References

[1] M.P. Harmer, Use of solid-solution additives in ceramic processing, in: W.D. Kingery (Ed.), Structures and Properties of MgO and Al_2O_3 Ceramics, American Ceramic Society, Columbus, OH, 1984 , pp. 679–696.
[2] A.X. Liang, I.W. Chen, Low-temperature sintering of with liquid-forming additives, J. Am. Ceram. Soc. 74 (8) (1991) 2011–2013.
[3] M.V. Swain, Materials science and technology, Structure and Properties of Ceramics, vol. 11, VCH, Weinheim, 1994, pp. 96–101.

[4] E.S. Lukin, N.A. Makarov, I.A. Dodonova, S.V. Tarasova, E.A. Bad'ina, N.A. Popova, New ceramic materials based on alumina oxide, Refract. Ind. Ceram. 42 (2001) 7–8.
[5] T. Ikegami, K. Kotani, Some of roles of MgO and TiO_2 in densification of a sinterable alumina, J. Am. Ceram. Soc. 70 (1987) 885–890.
[6] C. Toy, M. Demirci, S. Onurlu, M. Sadik Tasar, T. Baykara, Colloidal method for manganese oxide addition to alumina powder and investigation of properties, J. Mater. Sci. 30 (16) (1995) 4183–4187.
[7] D.H. Riu, Y.M. Kong, H.E. Kim, Effect of Cr_2O_3 addition on microstructural evolution and mechanical properties of Al_2O_3, J. Eur. Ceram. Soc. 20 (2000) 1475–1481.
[8] Y.Q. Wu, Y.F. Zhang, G. Pezzotti, J.K. Guo, Effect of glass additives on the strength and toughness of polycrystalline alumina, J. Eur. Ceram. Soc. 22 (2002) 159–164.
[9] R.D. Bagley, I.B. Cutler, D.L. Johnson, Effect of TiO_2 on initial sintering of Al_2O_3, J. Am. Ceram. Soc. 53 (3) (1970) 136–141.
[10] K. Hamano, C. Hwang, Z. Nagagawa, Y. Ohya, Yogyo Kyokai Shi/Journal of the Ceramic Society of Japan 94 (1986) 505–511 (in Japanese).
[11] D.S. Horn, G.L. Messing, Anisotropic grain growth in TiO_2-doped alumina, Mater. Sci. Eng. A 195 (1995) 169–178.
[12] Y.J. Park, N.M. Hwang, D.N. Yoon, Abnormal grain growth of faceted (WC) grains in a (Co) Liquid Matrix, Metall., Mater. Trans., A 27 (1996) 2809–2819.
[13] S.H. Lee, D.Y. Kim, N.M. Hwang, Effect of anorthite liquid on the abnormal grain growth of alumina, J. Eur. Ceram. Soc. 22 (2002) 317–321.
[14] O.S. Kwon, S.H. Hong, J.H. Lee, U.J. Chung, D.Y. Kim, N.M. Huang, Microstructural evolution during sintering of TiO_2/SiO_2-doped alumina: mechanism of anisotropic abnormal grain growth, Acta Mater. 50 (2002) 4865–4872.
[15] J.D. Hodge, The effect of particle size distribution on liquid phase sintering in alumina, in: C.A. Handwerker, J.E. Blendell, W.A. Kaysser (Eds.), Sintering of Advanced Ceramics, Ceramic Transactions, vol. 7, American Ceramic Society, Westerville, OH, 1990, pp. 415–435.
[16] Y.Q. Wu, Y.F. Zhang, X.X. Huang, J.K. Guo, Microstructural development and mechanical properties of self-reinforced alumina with CAS addition, J. Eur. Ceram. Soc. 21 (2001) 581–587.
[17] W.A. Kaysser, M. Sprissler, C.A. Handwerker, J.E. Blendell, Effects of a liquid phase on the morphology of grain growth in alumina, J. Am. Ceram. Soc. 70 (1987) 339–343.
[18] C.W. Park, D.Y. Yoon, Abnormal grain growth in alumina with anorthite liquid and the effect of MgO addition, J. Am. Ceram. Soc. 85 (6) (2002) 1585–1593.
[19] H. Erkalfa, Z. Misirli, T. Baykara, The effect of TiO_2 and MnO_2 on densification and microstructural development of alumina, Ceram. Int. 24 (1998) 81–90.
[20] T.Y. Chan, S.J. Liu, S.T. Lin, Effects of high concentrations of liquid phase and magnesia on the grain growth of alumina, Ceram. Int. 24 (1998) 617–625.
[21] J. Zhao, M.P. Harmer, Sintering of ultra-high-alumina doped simultaneously with MgO and FeO, J. Am. Ceram. Soc. 70 (1987) 860–866.
[22] E.R. Winkler, J.E. Sarver, I.B. Cutler, Solid solution of titanium dioxide in aluminum oxide, J. Am. Ceram. Soc. 49 (1966) 634–637.
[23] M. Sathiyakumar, F.D. Gnanam, Influence of MnO and TiO2 additives on density, microstructure and mechanical properties of Al_2O_3, Ceram. Int. 28 (2002) 159–200.
[24] W.D. Kingery, Densification during sintering in the presence of a liquid phase: I, theory, J. Appl. Phys. 30 (3) (1959) 301–306.
[25] W.D. Kingery, M.D. Narasimhan, Densification during sintering in the presence of a liquid phase: II, experimental, J. Appl. Phys. 30 (3) (1959) 307–310.
[26] S.J. Guo, Theory of Powder Sintering, Metallurgical Industry Press, Beijing, 2002, pp. 301–303.
[27] J. Rödel, A.M. Glaeser, Anisotropy of grain growth in alumina, J. Am. Ceram. Soc. 73 (11) (1990) 3292–3301.
[28] D.Y. Kim, S.M. Wiederhorn, B.J. Hockey, C.A. Handwerker, J.E. Blendell, Stability and surface energies of wetted grain boundaries in aluminum oxide, J. Am. Ceram. Soc. 77 (2) (1994) 444–453.